Improvements to Optical Track Association with the Direct Bayesian Admissible Region Method

Kohei Fujimoto
Texas A&M University, United States

Johannes Herzog and Thomas Schildknecht
Astronomical Institute of the University of Bern, Switzerland

Daniel J. Scheeres
University of Colorado-Boulder, United States

ABSTRACT

The direct Bayesian admissible region approach is an *a priori* state free measurement association and initial orbit determination technique. When this approach was initially applied to tracklets from a survey of geostationary objects taken at the Zimmerwald Observatory of the Astronomical Institute of the University of Bern, difficulties with both false associations and missed associations were encountered. In this paper, ideas to improve the association of tracklets are proposed and analyzed. It aims to close the loop on the short-arc optical track association problem by enhancing the survey strategy based on the association results and vice versa.

1. INTRODUCTION

The direct Bayesian admissible region (AR) approach proposed by Fujimoto and Scheeres is an *a priori* state free measurement association and initial orbit determination (IOD) technique [5]. Given a short-arc series of optical measurements, or a tracklet, a compact region in the range / range-rate space is defined based on a set of physical constraints such that all likely and relevant orbits are contained within it [11–13]. The AR is a uniform probability density function (PDF) whose support is this compact region. Multiple ARs may be propagated to a common epoch and an *a posteriori* PDF directly computed based on Bayes' rule.

Two distinct advantages of the direct Bayesian AR approach from the standpoint of reducing uncorrelated tracks (UCTs) are that only 2 tracklets are required as input (as opposed to 3 for geometric techniques that produce elliptic orbit solutions) and that observations from multiple nights are processed without any changes to the algorithm. During initial tests using actual tracklets of geosynchronous (GEO) belt objects taken at the Zimmerwald Observatory of the Astronomical Institute of the University of Bern (AIUB), however, two difficulties arose. The first were false associations due to the ambiguity in the number of revolutions made between observations, or multi-rev solutions. The second were missed associations due to the nominal assumption that the observation errors were small enough to be ignored. Consequently, a hybrid method was implemented, where the direct Bayesian results were passed to a least squares batch filter. Although the second difficulty was addressed well with this new method, not all multi-rev solutions were removed, partially because the observation strategy was not designed to explicitly include a second night (or further) of observations in the tracklet association process [7]. It was noted that the direct Bayesian approach is well-suited to explore alternative survey strategies because the association of tracklets is handled in a much more probabilistically straightforward way than other IOD techniques. Any changes to the current strategy would directly affect the *a posteriori* PDF in the state space without the need to assume an observation geometry, dynamical system, or the type of errors accounted for.

To this end, in this paper, ideas to further improve the association of tracklets involving the aforementioned hybrid method are proposed and analyzed. The outline of the paper is as follows. First, the basics of the direct Bayesian AR approach are outlined along with the least squares hybrid method and a new instant follow-up method which

associates 3 or more tracklets efficiently. Then, these ideas are tested with simulated data to better understand optimal observation cadences and tracklet lengths which reduce false associations. Finally, based upon the simulation results, a new survey strategy is devised, which is partially tested using optical observations from AIUB. This paper ultimately aims to close the loop on the too short-arc (TSA) optical track association problem by enhancing the survey strategy based on the association results and vice versa.

2. THE DIRECT BAYESIAN ADMISSIBLE REGION APPROACH

Various methods applying the AR concept to the TSA problem for resident space objects (RSOs) have been studied in recent years [2, 3, 10, 14, 21, 22]. In this paper, we define the AR as a PDF constrained in the range ρ and range-rate $\dot{\rho}$ directions via a few physical criteria such as that the orbit is elliptic, the object's range is within the sensing capabilities, and so on [5]. The angle and angle-rate, nominally in right ascension α and declination δ, at the epoch of a tracklet may be estimated via a least-squares fit of the tracklet data to a kinematic polynomial model in time t: e.g., for the right ascension

$$\alpha(t) = \alpha^0 + \dot{\alpha}^0(t - t^0) + \frac{1}{2}\ddot{\alpha}^0(t - t^0)^2, \tag{1}$$

where superscript 0 denotes the state at the tracklet epoch. These variables plus necessary parameters, such as the latitude ϕ and longitude Θ of the observation point, are referred to collectively as the attributable vector [10]. Thus, each point on the AR combined with its attributable vector corresponds one-to-one with a state that the observed object may have taken. Furthermore, the covariance from the least-squares fit may be incorporated in the AR to represent observational errors.

Suppose that, given some set of criteria $\mathcal{C}$, A is a compact set in state space $\mathcal{X}$ that meet $\mathcal{C}$. Then, the AR $F_{\mathcal{C}}[\mathbf{X}(t^0); \mathcal{Y}^0]$ is a PDF over $\mathcal{X}$ assigned to an attributable vector $\mathcal{Y}^0$ such that the probability p that the observed object exists in region $B \subset A$ at time t^0 is

$$p[\mathbf{X}(t^0)] = \int_B F_{\mathcal{C}}[\mathbf{X}(t^0); \mathcal{Y}^0] \mathrm{d}X_1^0 \mathrm{d}X_2^0 \ldots \mathrm{d}X_n^0, \tag{2}$$

where $\mathbf{X}(t^0) \in \mathcal{X}$ and

$$\mathbf{X}(t^i) \equiv \mathbf{X}^i = (X_1^i, X_2^i, \ldots, X_n^i). \tag{3}$$

Note that we impose $\int_A F_{\mathcal{C}}[\mathbf{X}(t^0); \mathcal{Y}^0] \mathrm{d}\mathbf{X}^0 = 1$. Here, as well as in the main analysis of this paper, the criteria are set to ensure that the AR encompasses most trackable object relevant to SSA while simultaneously filtering out highly eccentric orbits. Changing $\mathcal{C}$ allows one to be explicit about the types of orbits that are included in the analysis.

We may apply Bayes' rule directly to ARs in a common state space and at a common epoch τ; no reference state is required. To obtain the *a posteriori* PDF $h[\mathbf{X}(\tau)]$ based on 2 ARs $F_{\mathcal{C}}[\mathbf{X}^1; \mathcal{Y}^1]$ and $F_{\mathcal{C}}[\mathbf{X}^2; \mathcal{Y}^2]$,

$$h[\mathbf{X}(\tau)] = \frac{\{\mathcal{T}(\tau, t_1) \circ F_{\mathcal{C}}[\mathbf{X}^1; \mathcal{Y}^1]\}\{\mathcal{T}(\tau, t_2) \circ F_{\mathcal{C}}[\mathbf{X}^2; \mathcal{Y}^2]\}}{\int \{\mathcal{T}(\tau, t_1) \circ F_{\mathcal{C}}[\mathbf{X}^1; \mathcal{Y}^1]\}\{\mathcal{T}(\tau, t_2) \circ F_{\mathcal{C}}[\mathbf{X}^2; \mathcal{Y}^2]\} \mathrm{d}\mathbf{X}}, \tag{4}$$

where $\mathcal{T}(\tau, t^i)$ is a transformation that maps some PDF $f(\mathbf{X}^i, t^i)$ from time t^i to τ, and $\mathbf{X}(\tau) \equiv \mathbf{X}$. The domain of integration is over the entire state space. If the two tracklets associate, then $h[\mathbf{X}(\tau)] \neq 0$ for some value of $\mathbf{X}(\tau)$; a geometrical interpretation is that the *a posteriori* PDF is non-zero if the two ARs intersect. In general, any PDF may be used as input, such as density information from debris distribution models [16]. This approach is computationally feasible because each AR, ignoring observation errors, has codimension 4, making the problem extremely sparse. Furthermore, the sparseness also ensures that misassociations are highly unlikely unless the association is consistent with both the observation geometry and the dynamics [1]. From the Theorem of General Position, $h[\mathbf{X}(\tau)] = 0$ for all $\mathbf{X}$ generically if

$$\dim\left\{F_{\mathcal{C}}[\mathbf{X}^1; \mathcal{Y}^1]\right\} + \dim\left\{F_{\mathcal{C}}[\mathbf{X}^2; \mathcal{Y}^2]\right\} < \dim(\mathcal{X}), \tag{5}$$

where $\dim(\mathcal{X})$ is the dimension of the state space. Again, ignoring observation errors, $\dim\left\{F_{\mathcal{C}}[\mathbf{X}^i; \mathcal{Y}^i]\right\} = 2$ so the inequality holds for $\dim(\mathcal{X}) > 5$. The justification of associations is not at all related to the OD quality but rather solely to the geometry of the AR maps. Therefore, this method is robust with minimal tuning.

Finally, transformation $\mathcal{T}(\tau, t^i)$ is expressed analytically by means of a special solution to the Fokker-Planck equations valid for all deterministic dynamical models [6]. Given solution flow $\mathbf{X}(t) = \boldsymbol{\phi}(t; \mathbf{X}^i, t^i)$ to the dynamics

for initial conditions $\mathbf{X}^i$, the PDF $\mathcal{T}(\tau, t^i) \circ f(\mathbf{X}^i, t^i) = f(\mathbf{X}, \tau)$ is expressed as

$$f(\mathbf{X}, \tau) = f[\boldsymbol{\phi}(\tau; \mathbf{X}^i, t^i), \tau] = f(\mathbf{X}^i, t^i) \left| \frac{\partial \mathbf{X}(\tau)}{\partial \mathbf{X}^i} \right|^{-1}, \tag{6}$$

where $|\cdot|$ indicates the determinant operator.

2.1. Least Squares Hybrid Method

We now present an outline of the hybrid algorithm [7]. First, admissible regions are computed for each attributable vector in the Poincaré orbit element space ($\mathfrak{L}$, $\mathfrak{l}$, $\mathfrak{G}$, $\mathfrak{g}$, $\mathfrak{H}$, $\mathfrak{h}$), which are a canonical counterpart to equinoctial elements [23]. The admissible region is divided into 375,000 subsets (750 units of discretization in the range-direction $\times$ 500 units in the range-rate) and each subset linearly extrapolated. The Poincaré space, and consequently ARs, are discretized such that the bounds of the state space are

$$\mathbf{X}_{\min} = (4.5285, 0, -3, -3, -4, -4) \tag{7}$$

$$\mathbf{X}_{\max} = (14.110, 6.2832, 3, 3, 4, 4), \tag{8}$$

where the units are in Earth radii - kg - hr. The bin size is set such that the sides are $1.1052 \cdot 10^{-2}$ ($\mathfrak{L}$), $1.7453 \cdot 10^{-2}$ ($\mathfrak{l}$), $1.6667 \cdot 10^{-2}$ ($\mathfrak{G}$, $\mathfrak{g}$), and $2.2222 \cdot 10^{-2}$ ($\mathfrak{H}$, $\mathfrak{h}$) for a total of 5.2424×10^{15} bins over the entire space. This resolution corresponds to approximately 100 km in the semi-major axis direction and 1 degree in the mean anomaly direction. The admissible region are propagated to a common epoch, which is chosen to be the tracklet epoch of the first tracklet, under two-body dynamics. The two-body assumption is made only to simplify the problem and is not central to the direct Bayesian technique.

If, for some pair of tracklets, a non-zero *a posteriori* PDF is returned, a bank of least squares batch filters are run such that the reference state of each filter is the centroid of each bin where $h[\mathbf{X}(\tau)] > 0$ transformed into the J2000 cartesian space. In this paper, we assume that no *a priori* information exists; if desired, the *a priori* covariance may be set to approximate $h[\mathbf{X}(\tau)]$. The assumed observation error is set to 1.2 arcsec 1-σ. The observation-state relationship and corresponding linear partials matrix assume a spherical Earth. In order to minimize multi-rev solutions, if the $O - C$ residuals of the least squares estimate exhibit an obvious linear bias, then assuming that the observation errors are modeled as white noise, these solutions are rejected. That is, for the set of filters that converge, if

1. the root mean square (RMS) of the residuals for either RA/DEC is less than 3.6 arcsec over both tracklets **AND**
2. **IF** the RMS of the residuals for either RA/DEC of either tracklet is greater than 1.2 arcsec, the p-value of the model utility test for either RA/DEC residuals of either tracklet is greater than 0.01,

only then are the tracklets confirmed to be associated, and the state estimate with the smallest $O - C$ residual RMS is added to the object catalogue. The specific tolerances are chosen to best describe the observational capabilities of the Zimmerwald SMall Aperture Robotic Telescope (ZimSMART), from which we take observations in this paper [8, 9].

2.2. Instant Follow-Up Method

Simultaneously associating 3 or more tracklets is beneficial in reducing the number of multi-rev solutions; the more tracklets are associated at once, the less likely it is for a fictitious yet consistent solution to exist [15]. As objects are oftentimes observed much more than twice per night, the observational data to implement such a method are available. Computational burden, however, increases significantly. If n tracklets were to be associated l at a time, the runtime will scale as n^l. With potentially thousands of tracklets gathered every night, the problem quickly becomes intractable even with small values for l [19].

To avoid a potential surge in computation time, one may initially test associations one-by-one as pairs, but when an association is detected, the *a posteriori* solution may be immediately associated in all-on-all fashion against the remaining tracklets. If one desires to associate more than 3 tracklets, then the additional tracklets found to associate with the tracklet pair may further be combined to form tracklet sets of a specified length. In this new method, which we refer to as instant follow-up, the all-on-all association takes minimal computational burden as the support of the *a posteriori* PDF of the AR association is very small. It also leverages the fact that many branches of the combinatorial tree structure of observations may be pruned with just tracklet pairs, where the runtime scales as n^2. As such, the direct Bayesian approach ends up being more computationally efficient overall than conventional techniques even though it may be slower per individual association run.

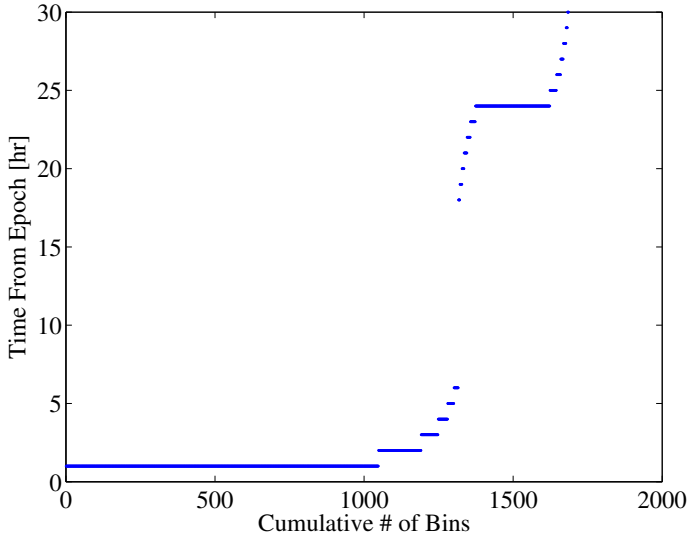

Figure 1: The cumulative number of solution bins separated by contributions from each tracklet epoch.

3. SIMULATIONS ON OBSERVATION CADENCE AND LENGTH

In order to harness the benefits of the direct Bayesian approach of 2-tracklet association / IOD over multiple nights but simultaneously reduce any false associations, one must revisit the strategy from which the observations originate. Two particular trade spaces of the survey are studied in this paper; the observation cadence and tracklet length. Tracklets from AIUB's ZimSMART are simulated using a MATLAB script. The number of images per tracklet, the time between images in each tracklet, and the time between tracklets themselves can be adjusted arbitrarily. The simulation epoch is 8 Aug 2012 22:59:8.634 UCT. Here, observations are assumed to have Gaussian zero-mean error with a standard deviation of 0.7 arcsec. Earth shadowing and other lighting phenomena are ignored for simplicity.

3.1. 2-Tracklet Association

We first attempt to better understand the effect observation cadence has on the association process using only 2 tracklets. We consider a scenario where one geostationary object is observed at the simulation epoch and then again at either 1, 2, . . . , 6, 18, 19, . . . , 29 or 30 hours after epoch. Observations taken 18 – 23 hours after epoch are included, even though they occur before sunset, because we assume that their relative geometry with respect to the epoch observation would not change had the epoch been 1 – 6 hours later. Tracklet length is fixed to 7 images over 77 seconds. The orbital elements at epoch are given as

$$(a, e, i, \Omega, \omega, M) = (42165.325216, 0.000379, 0.069, 87.544, 43.733, 204.572) \tag{9}$$

in units of km for length and deg for angles. Figure 1 shows the solution accuracy (i.e. number of discretization bins that the *a posteriori* PDF occupies) for the direct Bayesian AR only IOD. As expected, a large region of the state space is consistent with the tracklet pair when the time gap between observations is small and when it is 24 hours. The latter suggests that a GEO-belt survey strategy with the exact same sequence over consecutive nights should be avoided.

Next, to determine the effect that tracklet length has on reducing false associations, we consider a scenario where one geosynchronous object (GEO1) is observed at the simulation epoch but a separate geostationary object (GEO2) is subsequently observed either 1, 2, . . . , 6, 18, 19, . . . , 29 or 30 hours after epoch. All tracklet pairs, thus, must not associate. The orbital elements at epoch are given as

$$\text{GEO1: } (a, e, i, \Omega, \omega, M) = (42246.925164, 0.000466, 0.030, 61.955, 303.364, 336.173) \tag{10}$$

$$\text{GEO2: } (a, e, i, \Omega, \omega, M) = (42165.325216, 0.000379, 0.069, 87.544, 43.733, \ \ 204.572) \tag{11}$$

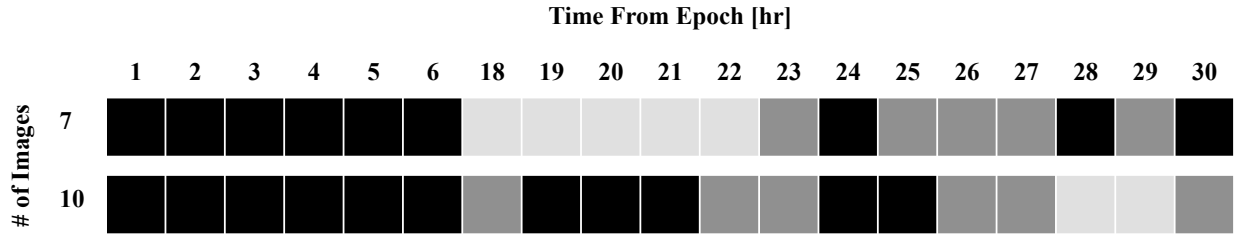

Figure 2: Rejection of false positive solutions as a function of both the "Time From (simulation) Epoch" and the "number (#) of images" per tracklet. Black boxes are tracklet pairs rejected due to the residual RMS criterion, dark grey boxes are pairs rejected due to the p-value criterion, and a light grey boxes are pairs falsely associated.

in units of km for length and deg for angles. In addition to the nominal tracklet with a length of 77 seconds, a longer tracklet with 11 images over 110 seconds is tested. Figure 2 shows observation epochs for which tracklet pairs were falsely associated. Even with the longer simulated tracklet, it was not possible to remove all drifter-type false positive solutions. Further tests suggest that tracklets of $\sim$3 minutes or longer are required for both the angle-rate estimate to be good enough and the residual biases to be apparent enough for the p-value criterion to provide consistent performance. Such long tracklets, however, are impractical not only because they significantly reduce the number of observations that may be made per night but also because they may negatively affect tracklet detection software, which often rely on linear models for RSO motion. Therefore, using the residuals alone as the basis for multi-rev solution rejection is not recommended when only 2 tracklets are associated. 2-tracklet solutions which especially span multiple nights should be treated as provisional unless more associating observations are available or other non-kinematic measurement types, such as spectral and photometric data, are incorporated in the analysis [17, 18, 20].

3.2. 2-Tracklet Association + 2-Tracklet Instant Follow-Up

As indicated in the analysis above, one can be more confident regarding the validity of an association when 3 or more observations are processed simultaneously. It is of interest, then, to study the effect of observation cadence on the precision and estimated accuracy of the IOD solution for these larger tracklet sets. Here, the first scenario in Section 3.1 is considered again, but this time, the *a posteriori* solution of the association between tracklets taken 0 and 4 hours after epoch is then further associated with 2 more tracklets in instant follow-up fashion. Tracklets taken 18 – 23 hours epoch are no longer included in the analysis as these observations now must occur before sunset. Figure 3 is a contour plot of the state estimate precision (estimated $-$ truth) and accuracy (covariance) at epoch as a function of the timing of the instant follow-up tracklets. Only the covariance in the radial direction is highlighted here as it is the least observable direction for optical observations.

Comparing the clusters in the bottom left (all 4 tracklets taken during the second night) and top left (3 tracklets taken during the first night + 1 tracklet taken during the second night) corners, we find that, as expected, observations spanning 2 nights result in improved IOD accuracy by up to an order of magnitude. The same cannot be said, however, of the cluster in the top right corner (2 tracklets taken from each night) as the IOD accuracy is, in some cases, worse than processing observations from a single night. In addition to poor observation geometry, these inaccurate solutions are caused by the large state uncertainties of 2-tracklet solutions; the semi-major axis of the position uncertainty ellipsoid grows from $\sim 10^2$ km at epoch to $\sim 10^3$ km after 24 hours of linear propagation. Even though dynamics adds information to observations spaced further out in time, the RSO's state is not estimated well enough for this effect to trump the temporal growth in uncertainty. For the most accurate tracklet association and IOD results, then, it is preferable that RSOs be observed at least 3 times per night.

4. CORROBORATION WITH OPTICAL DATA

We now determine the effectiveness of the instant follow-up method with optical data from AIUB's ZimSMART. Detailed measurement parameters are found in Table 1. 196 tracklets taken on August 9, 2013 and 242 the following night are associated without any *a priori* information using 2 tracklets (direct Bayesian only OR least squares hybrid) and 2 tracklets + 1 tracklet instant follow-up. The direct Bayesian algorithm is applied only to tracklets separated in

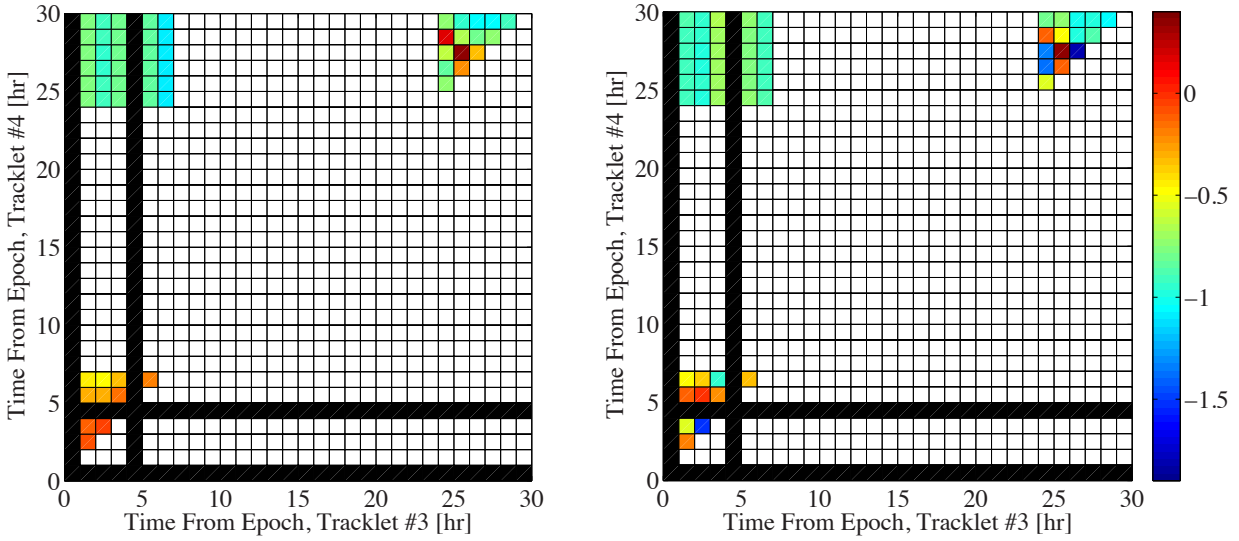

Figure 3: Log_{10} of the standard deviation of the state estimate in the radial direction (left) and of the state estimate precision (right) for the least squares hybrid method with 2-tracklet instant follow-up. Direct Bayesian admissible region solution based on tracklets at 0 and 4 hours after epoch; these times are filled in black.

Table 1: Parameters for the data set used in this example. The number of objects detected is based on AIUB correlation results.

Parameter	**Value**
Epoch of initial field	Aug 9, 2013 20:14:11.70 UTC
Epoch of final field	Aug 11, 2012 00:27:24.87 UTC
Total # of fields	147
Total # of tracklets	438
Total # of objects detected	63
# of objects detectable with 2-tracklet association	63
# of objects detectable with instant follow-up	17

time by 12 hours or greater. Instant follow-on tracklets are searched for 0 – 10 hours after the epoch of the first tracklet in the associated pair. The observations are made on two stripes of constant right ascension to the east of the shadow of the Earth and two to the west. The stripes are moved accordingly if they overlap with the Moon or the Milky Way. This strategy has the advantage that the illumination conditions are nearly optimal.

Association results are compared against AIUB's internal tracklet correlation and association code: tracklets are first geometrically correlated with the TLE catalogue, and any leftover UCTs are associated with a circular orbit IOD plus subsequent least squares fit [4,8,9]. Hypotheses generated by the direct Bayesian-related strategies are categorized into **Type I** (all tracklets associated are correlated to the same object by the AIUB code; likely true positive solution), **Type II** (one or more tracklets associated are correlated to separate objects by the AIUB code; likely false positive solution), or **Type III** (one or more tracklets associated are uncorrelated by the AIUB code; new association candidate). Furthermore, RSOs detected by the AIUB code are categorized as **Fully Detected** (all tracklets correlated to the RSO are similarly associated by the direct Bayesian-related method), **Partially Detected** (some correlated tracklets are associated), and **Not Detected** (no correlated tracklets are associated).

Table 2 is a summary of the results. The simplest 2-tracklet direct Bayesian only association succeeds in detecting all of the objects that the AIUB code did. Although it prunes over 90% of tracklet pair hypotheses as unassociated, a majority of the remaining hypotheses are likely false positive solutions since there are nearly 60 times more hypothe-

Table 2: Association results using 2 tracklets (Direct Bayesian only OR Least Squares hybrid) and 2 tracklets + 1 tracklet instant follow-up. Listed are the ratio of hypotheses for each type (Type I – III), the total number of hypotheses (Total), the ratio of hypotheses pruned as unassociated (Pruned), and the number of RSOs detected out of those detected by existing AIUB code (Fully Det., Part. Det., Not Det.).

Assoc. Method	**Type I**	**Type II**	**Type III**	**Total (Pruned)**	**Fully Det.**	**Part. Det.**	**Not Det.**
Direct Bayesian only	3.1%	17.5%	79.4%	3658 (92.3%)	62	1	0
LS hybrid	3.9%	18.8%	77.2%	2789 (94.1%)	61	1	1
Inst. follow-up	39.2%	7.8%	52.9%	51 (99.9%)	14	1	2

ses than objects detected by the AIUB code. The addition of the least squares step increases the number of hypotheses pruned by about 2 percentage points. From the perspective of reducing false positive solutions, the current implementation of instant follow-up method is effective, raising the ratio of Type I solutions by an order of magnitude compared to the 2-tracklet association results while simultaneously rejecting 99.9989% of hypotheses. It is also computationally more efficient to add a third tracklet to an associating pair rather than evaluating all combinations of tracklet triplets because, again, over 90% of triplets are automatically rejected after the 2-tracklet direct Bayesian association. Nonetheless, many RSOs are revisited with an approximately 24-hour time gap with only two tracklets associated in the first night, suggesting that IOD solution accuracies may be poor. Therefore, one may be able to further decrease false associations by changing the survey strategy.

5. PROPOSED SURVEY IMPROVEMENTS

To summarize the recommendations made in Section 3, an observation strategy that explicitly takes into account 2 or more nights of observations is preferable. From the standpoint of convergence, it is important to avoid taking the exact same strategy over consecutive nights and preferable to take at least 3 observations of each object during the first night. As discussed in Section 4, the instant follow-up method is a viable way to efficiently search for multiple associating tracklets. In this section, a new survey strategy is devised that reflects said recommendations and is suited for direct Bayesian-related association methods. We begin by defining 6 stripes (or fences) in the azimuth (Az) - elevation (El) space as shown in Figure 4, spanning approximately 78 – 102 degrees in Az. Each stripe contains 6 fields of size 3.6 deg $\times$ 3.6 deg; i.e., the field of view of ZimSMART. The span in El should be determined based on the distribution of geostationary (GEO) belt objects in order to maximize object detections. Label each stripe, from lowest Az to highest, as 1, 2, 3, . . . , 6. We will further group the stripes into 2 groups, I and II:

Group I Stripes 1, 3, and 5

Group II Stripes 2, 4, and 6.

The observation of these stripes takes place over 3, preferably consecutive, nights. Each night is divided into 3 segments which are 100 minutes long, totaling to 300 minutes = 5 hours of observation time per night. Thus, sufficient time for preparation, calibration, and other routine maintenance tasks is secured. During the first 100 minutes of Night 1, stripes in Group I are observed. Each stripe within Group I should be observed 3 times

$$1 - 3 - 5 - 1 - 3 - 5 - 1 - 3 - 5.$$

Assuming each field takes 77 seconds to observe and consequently each stripe $\sim$ 10 minutes to observe, at least 10 minutes are reserved as margin for maintenance needs and other contingencies. During the next 100 minutes, Group II is observed in a similar fashion; 3 stripes are observed 3 times each. During the final 100 minutes, Group I is revisited and observed in the same sequence as before. For Night 2, the same sequence is employed as Night 1 except that Group II is observed first, then I, then back to II. Finally, for Night 3, the exact same sequence is employed as Night 1. Table 3 is a summary of the entire strategy.

The benefits of the proposed survey strategy is as follows. The Az-El region included in Group I is observed 4 – 6 hours then 26 – 28 hours after epoch, nominally resulting in better IOD convergence compared to a repeating single-night strategy. Revisits to Group II are similarly shifted between consecutive nights. Additionally, for geostationary objects, a maximum of 6 tracklets will be output during Night 1 alone for Group I or Night 2 for Group II; thus, there

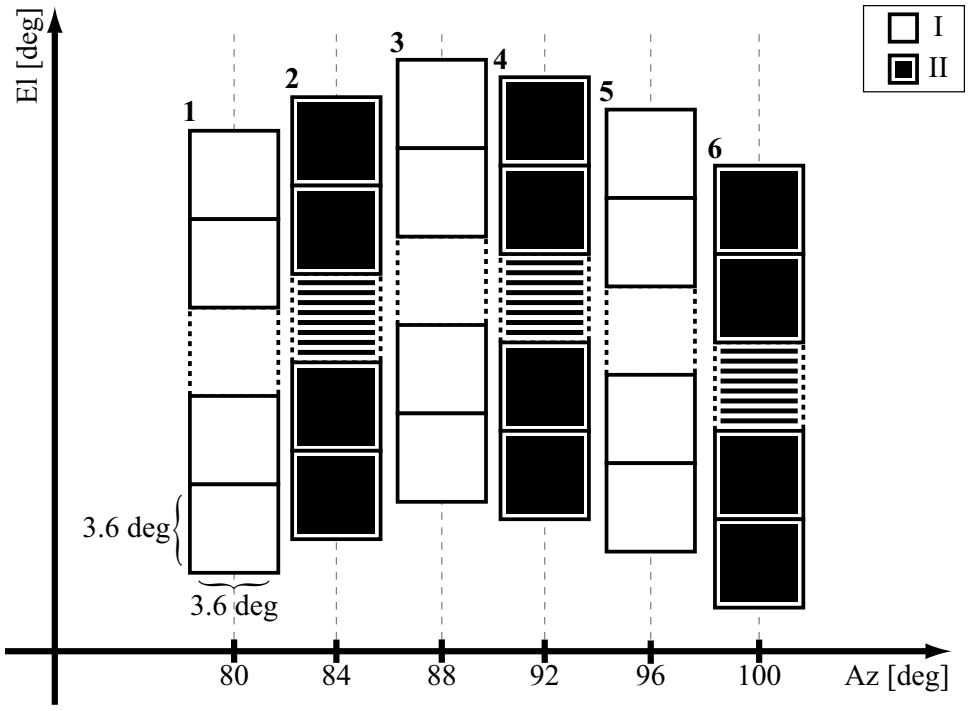

Figure 4: Graphical representation of stripes and stripe groups defined in the proposed observation strategy. Each rectangle, consisting of several square fields, represent stripes with their stripe number indicated on the top left corner. Stripes in Group I are filled in white while those in Group II are filled in black.

should be a sufficient number of observations to ensure good IOD convergence. Finally, the quality of association and IOD solutions may be inferred, to some extent, by the groups from which tracklets are taken. For example, following the prime notation introduced in Table 3, one would be more confident regarding solutions combining tracklets from Groups I, I', and I", say, than solutions from Groups I and II only. Consequently, there exists a structural order in which tracklets should be combined based upon expected solution quality.

6. CONCLUSIONS

In this paper, improvements are proposed for both the direct Bayesian admissible region method of optical measurement association and the survey strategy from which measurements are taken. With the direct Bayesian method, a vast majority of track association hypothesis pairs are pruned, meaning that adding tracks to the hypotheses in order to reduce false positive solutions is computationally insignificant compared to an exhaustive search. Optical data from the Astronomical Institute of the University of Bern corroborates this instant follow-up methodology. Furthermore, by explicitly including observations from multiple nights in the association process, simulations show that survey strategies should not repeat nightly if one were to maximize state estimate accuracy. Based on these findings, a new survey strategy is proposed. Future work is to implement said strategy and quantitatively assess its performance.

ACKNOWLEDGEMENTS

The authors would like to thank the researchers and staff of AIUB and the Zimmerwald Observatory who provided the optical data. A special acknowledgement goes to Martin Ploner, the technical head.

Table 3: Overview of the proposed observation strategy. Numbers in parenthesis indicate the required time for the particular task including margins for contingency. One prime indicates the first time a group has been revisited, two primes the second, and so on.

Night	**Group**	**Stripe**
1 (480)	I (100)	1 (10)
		3
		5
		1
		3
		5
		1
		3
		5
	II (100)	2
		4
		6
		⋮
	I' (100)	1
		3
		5
		⋮
2 (480)	II'	⋮
	I"	⋮
	II"	⋮
3 (480)	I"'	⋮
	II"'	⋮
	I""	⋮

References

[1] J. S. Carter. *How Surfaces Intersect in Space: An introduction to topology*. World Scientific, Singapore, second edition, 1995. pp. 277.

[2] K. J. DeMars and M. K. Jah. Initial orbit determination via gaussian mixture approximation of the admissible region. 2012. Presented at the AAS/AIAA Spaceflight Mechanics Meeting, Charleston, SC, AAS 12-260.

[3] D. Farnocchia, G. Tommei, A. Milani, and A. Rossi. Innovative methods of correlation and orbit determination for space debris. *Celestial Mechianics and Dynamical Astronomy*, 107(1-2):169–185, 2010.

[4] C. Früh, T. Schildknecht, R. Musci, and M. Ploner. Catalogue correlation of space debris objects. In *5th European Conference on Space Debris*, 2009.

[5] K. Fujimoto and D. J. Scheeres. Correlation of optical observations of earth-orbiting objects and initial orbit determination. *Journal of Guidance, Control, and Dynamics*, 35(1):208–221, 2012.

[6] K. Fujimoto and D. J. Scheeres. Non-linear propagation of uncertainty with non-conservative effects. 2012. Presented at the *AAS/AIAA Spaceflight Mechanics Meeting*, Charleston, SC. AAS 12-263.

[7] K. Fujimoto, D. J. Scheeres, J. Herzog, and T. Schildknecht. Applying the direct Bayesian admissible region approach to the association of GEO belt optical observations. 2013. Presented at the *29th International Symposium on Space Technology and Science*, Nagoya, Japan, 2013-r-19.

[8] J. Herzog, C. Früh, and T. Schildknecht. Build-up and maintenance of a catalogue of GEO objects with ZimSMART and ZimSMART 2. 2010. Presented at the *61st International Astronautical Congress*, Prague, Czech Republic. IAC-10.A6.5.2.

[9] J. Herzog, T. Schildknecht, and M. Ploner. Space debris observations with ZimSMART. 2011. Presented at the *European Space Surveillance Conference*, Madrid, Spain.

[10] J. M. Maruskin, D. J. Scheeres, and K. T. Alfriend. Correlation of optical observations of objects in earth orbit. *Journal of Guidance, Control and Dynamics*, 32(1):194–209, 2009.

[11] A. Milani, G. Gronchi, Z. Knežević, M. E. Sansaturio, and O. Arratia. Orbit determination with very short arcs ii. identifications. *Icarus*, 179:350–374, 2005.

[12] A. Milani, G. Gronchi, M. Vitturi, and Z. Knežević. Orbit determination with very short arcs. i admissible regions. *Celestial Mechanics and Dynamical Astronomy*, 90:57–85, 2004.

[13] A. Milani and Z. Knežević. From astrometry to celestial mechanics: orbit determination with very short arcs. *Celestial Mechanics and Dynamical Astronomy*, 92:118, 2005.

[14] A. Milani, G. Tommei, D. Farnocchia, A. Rossi, T. Schildknecht, and R. Jehn. Correlation and orbit determination of space objects based on sparse optical data. *Mon. Not. R. Astron. Soc.*, 417:2094–2103, 2012.

[15] R. Musci, T. Schildknecht, and M. Ploner. Orbit improvement for GEO objects using follow-up observations. *Advances in Space Research*, 34:912–916, 2004.

[16] M. Oswald, S. Stabroth, C. Wiedemann, P. Wegener, H. Klinkrad, and P. Vörsmann. ESA's MASTER 2005 debris environment model. *Advances in the Astronautical Sciences*, 123(1):811–824, 2006.

[17] T. Schildknecht, C. Früh, J. Herzog, A. Hinze, and A. Vananti. AIUB efforts to survey, track, and characterize small-size objects at high altitudes. 2010. Presented at the *Advanced Maui Optical and Space Surveillance Technologies Conference*, Wailea-Maui, HI.

[18] T. Schildknecht, A. Vananti, H. Krag, and C. Erd. Reflectance spectra of space debris in GEO. 2009. Presented at the *Advanced Maui Optical and Space Surveillance Technologies Conference*, Wailea-Maui, HI.

[19] P. W. Schumacher, Jr., M. Wilkins, and C. Roscoe. Parallel algorithm for track initiation for optical space surveillance. 2013. Presented at the *6th European Conference on Space Debris*, Darmstadt, Germany.

[20] R. L. Scott and B. Wallace. Small-aperture optical photometry of Canadian geostationary satellites. *Can. Aeronaut. Space J.*, 55(2):41–53, 2009.

[21] J. A. Siminski, O. Montenbruck, H. Fiedler, and M. Weigel. Best hypothesis search on iso-energy-grid for initial orbit determination and track association. 2013. Presented at the *23rd AAS/AIAA Spaceflight Mechanics Meeting*, Kauai, HI. AAS 13-239.

[22] G. Tommei, A. Milani, and A. Rossi. Orbit determination of space debris: admissible regions. *Celestial Mechanics and Dynamical Astronomy*, 97:289–304, 2007.

[23] D. Vallado. *Fundamentals of Astrodyamics and Applications*. Microcosm Press, Hawthorne, CA, third edition, 2007.